Available online at www.sciencedirect.com
ScienceDirect
Materials Chemistry and Physics 102 (2007) 249–254
MATERIALS CHEMISTRY AND PHYSICS
www.elsevier.com/locate/matchemphys

Fabrication and photovoltaic properties of self-assembled sulfonated polyaniline/TiO_2 nanocomposite ultrathin films

Xiuqin Zhang, Guolun Yan, Hanming Ding *, Yongkui Shan

Department of Chemistry, East China Normal University, Shanghai 200062, China

Received 15 November 2005; received in revised form 18 September 2006; accepted 27 December 2006

Abstract

Two kinds of TiO_2/sulfonated polyaniline (SPAn) nanocomposite ultrathin films were fabricated by layer-by-layer (LBL) self-assembly technique on various solid surfaces. One was fabricated with self-doped sulfonated polyaniline (SD-SPAn) and TiO_2 sol, and another was with externally (HCl)-doped sulfonated polyaniline (ED-SPAn) and $TiCl_4$. The linear growth of both the LBL films was proved by UV–vis spectroscopy. The ordered multilayer films were subsequently characterized by atomic force microscopy, cyclic voltammetry, and photoelectrochemical measurement. Their structure, electrochemical and photoelectrochemical properties were comparatively investigated. The morphology of ED-SPAn/TiO_2 LBL films is evener and smoother than that of SD-SPAn/TiO_2 LBL films. Two kinds of LBL films have different electrochemical behaviours, and ED-SPAn/TiO_2 LBL films show a stabler but slower photocurrent response than SD-SPAn/TiO_2 LBL films.

Keywords: Titanium oxide; Sulfonated polyaniline; Self-assembly; Photovoltaic properties

1. Introduction

Nanocomposites of conducting polymer/metal oxide have attracted much attention in recent years due to their wide range of applications [1–4]. Among various conducting polymers, polyaniline (PANI) has been attracted great interest because of its superior capabilities and wide applications, and has been successfully utilized in preparation of different nanocomposites with various oxides, such as TiO_2, SiO_2, V_2O_5 and Fe_2O_3 [5–10]. Among these oxides, TiO_2 has received particular attention due to its good stability, environment-friendliness and interesting semiconducting property. Various PANI–TiO_2 nanocomposites have been prepared by using chemical polymerization or electrochemical polymerization of aniline in the presence of TiO_2 nanocolloidals, and have found applications in electrochromic devices [11], p–n heterojunction diodes [12], rectifier [13], gas sensor [14], high piezoresistivity [15], electrorheological response [16], cathode electrode in rechargeable battery [17], photoelectrochemical devices [5,6,11,18]. Polyaniline–TiO_2 nanocomposites were usually prepared in the form of thin film, powder, sphere [19,20], or tube [21]. In most of these cases, the nanocomposites were further used in various applications in their thin-film form. However, the insolubility of PANI in most common solvents increases the difficulties to prepare PANI–TiO_2 nanocomposite thin films.

In order to improve the solubility of PANI, several water-soluble polyanilines in doped conducting form have been synthesized by introducing protonic acid into the chains, in which sulfonated polyanilines are mostly investigated [22–26]. Sulfonated polyaniline (SPAn) can be synthesized through the sulfonation of emeraldine base to get its protonic acid self-doped form [22,23]. The self-doped sulfonated polyaniline (SD-SPAn) is insoluble in water, but can be dissolved in alkali aqueous solution. Externally doped sulfonated polyaniline (ED-SPAn) can be synthesized through a direct sulfonation of emeraldine salts with chlorosulfonic acid in an inert solvent, which is water-soluble [24,25].

In our current work, two kinds of SPAn were employed to prepare SPAn–TiO_2 nanocomposite ultrathin films by using layer-by-layer (LBL) self-assembly technique. One was fabricated with self-doped sulfonated polyaniline (SD-SPAn) and TiO_2 colloidals based on alternately electrostatic adsorption [27], and another was fabricated with externally doped sulfonated polyaniline (ED-SPAn) and $TiCl_4$ in toluene–methanol mixture through the surface sol–gel process [28]. In both the cases, the morphology of thin films, the size of TiO_2 nanoparticles and

* Corresponding author. Tel.: +86 2162232414; fax: +86 2162232414.
E-mail address: hmding@chem.ecnu.edu.cn (H. Ding).

0254-0584/$ – see front matter © 2007 Elsevier B.V. All rights reserved.
doi:10.1016/j.matchemphys.2006.12.013

arrangement of SPAn in film can be effectively controlled, which are important factors in their potential applications.

2. Experimental

2.1. Materials and instruments

The emeraldine base (EB) of polyaniline was synthesized using the method similar to Yeh et al. [29]. The synthesis of SD-SPAn and ED-SPAn followed the procedures of Yue et al. [22,23] and Ito et al. [24], respectively. Tetrabutyl titanate ($Ti(OC_4H_9)_4$), titanium chloride ($TiCl_4$), poly(diallydimethylammonium chloride) (PDDA) (average molecular weight, 200,000–350,000, 20 wt.% in water) were purchased from Aldrich and used as received. Quartz plate, silicon wafer, and indium-tin oxide (ITO) glass were carefully cleaned and treated before they were used as the substrates for the fabrication of LBL films.

The UV–vis spectra were recorded on a Unican UV–vis spectrophotometer. AFM images were obtained with an AJ-III atomic force microscopy. The electrochemical and photoelectrochemical measurements were carried out on a CH Instrument 660 electrochemical workstation.

2.2. Film assembling

SD-SPAn was dissolved in ammonia solution at concentration of 0.25 mg ml^{-1} and was then adjusted to about pH 9 with dilute HCl solution. ED-SPAn was dissolved in deionized water at concentration of 0.25 mg ml^{-1} and was then adjusted to about pH 1.5 with dilute HCl solution. TiO_2 sol was prepared by dissolving 4 ml $Ti(C_4H_9O)_4$ in 20 ml ethanol and slowly adding into 150 ml deionized water in presence of 2 ml HNO_3. The solution was stirred at 50 °C for 3 h and then was adjusted to about pH 2 with dilute NH_4OH solution. $TiCl_4$ solution was prepared in 1:1 (v/v) toluene–methanol mixture in a concentration of 0.1 M.

All the substrates were treated as hydrophilic according to usual procedure and kept in deionized water prior to their use for LBL deposition. For the hydrophilic surfaces, the substrates were previously immersed in PDDA solution. One pre-treated substrate was immersed alternately in SD-SPAn solution and TiO_2 sol for 10 min and subsequently rinsed with deionized water and dried, in order to get the SD-SPAn/TiO_2 LBL films. In another case, one pre-treated substrate was immersed alternately into ED-SPAn and $TiCl_4$ toluene–methanol solutions and subsequently rinsed with deionized water and methanol and then dried. The ED-SPAn/TiO_2 LBL films were finally obtained.

2.3. Electrochemical and photoelectrochemical experiments

A three-electrode system was employed in all these experiments. ITO glasses modified with nanocomposite multilayer films were used as working electrodes. The counter electrode is platinum wire, and the reference is a saturated Ag/AgCl electrode. 0.1 M KCl solution was used as a support electrolyte. A 500 W halogen lamp was used as an irradiation source, and the distance from the source to working electrode is about 30 cm.

3. Results and discussion

3.1. Film fabrication

The SD-SPAn/TiO_2 LBL films were prepared by alternately electrostatic adsorption process. When the self-doped conducting form of SD-SPAn (Scheme 1A) was dissolved in ammonia solution, SPAn exists as ammonium salt, which is insulating (Scheme 1B) [23]. The films of the insulating ammonium salt of SPAn can spontaneously revert to the self-doped conducting form through dissociation of NH_4^+ into NH_3 and H^+, or with acidic media. A pre-treated positively charged substrate was firstly immersed in SD-SPAn solution and adsorbed the negatively charged sulfonated groups of SD-SPAn, and consecutively adsorbed TiO_2 sol nanoparticles that bring positive charges.

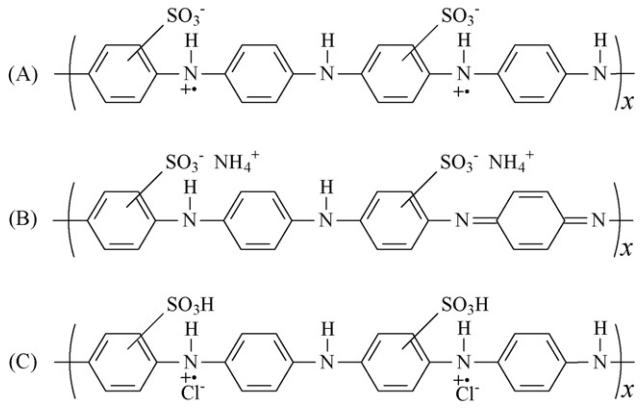

Scheme 1. Chemical structure of sulfonated polyamine at various states: (A) self-doped (SD-SPAn) [22,23], (B) ammonium salt, and (C) doped with HCl (ED-SPAn) [24].

The LBL films of ED-SPAn and TiO_2 were prepared by sequential adsorption/hydrolysis/condensation process [28]. The driving force for fabrication of the LBL films was the interactions between sulfonic acid groups and titanium species. When ED-SPAn films were immersed into a $TiCl_4$ toluene–methanol solution, since $TiCl_4$ reacted with methanol, titanium chloromethoxides reacted with the sulfonic acid groups in ED-SPAn (Scheme 1C) and sulfonate groups were chelated to titanium atoms through ester bonding [2]. The activated TiO_2 surface was then attached to sulfonic groups when such film was re-immersed in ED-SPAn solution.

3.2. UV–vis spectra

UV–vis spectroscopy was initially used to monitor the growth of these LBL multilayers. In SD-SPAn aqueous solution, the peaks at 318 and 567 nm are ascribed to the $\pi \rightarrow \pi^*$ transition and the "exciton" transition [22,23]. When SPAn becomes its self-doped form, there are three absorption bands at 320, 435 and 850 nm. The former is assigned to the $\pi \rightarrow \pi^*$ transition, and the latter two bands are ascribed to the polaron-π^* and π-polaron transition of the conducting form, respectively [23]. Fig. 1a shows the UV–vis absorption spectra of 2, 4, 6, 8 and 10 bilayers of the SD-SPAn/TiO_2 films assembled on quartz plates. The peak at 215 nm is attributed to TiO_2 nanoparticles, and the absorption at 245 nm can be assigned to the $\pi \rightarrow \pi^*$ transition of polyaniline backbone. The weak peak at ~600 nm can be ascribed to the molecular "exciton" transition, which indicates that SPAn exists as emeraldine base in the SD-SPAn/TiO_2 LBL films.

In the case of the ED-SPAn/TiO_2 LBL films, the peak at 207 nm is assigned to TiO_2 (Fig. 1b), which has a blue shift of about 8 nm relative to its counterpart in the SD-SPAn/TiO_2 LBL films. This fact suggests that the size of TiO_2 nanoparticles in the ED-SPAn/TiO_2 LBL films is smaller than that in the SD-SPAn/TiO_2 LBL films, according to Brus's proposed model [30]. The absorption at 260 nm is assigned to the $\pi \rightarrow \pi^*$ transition

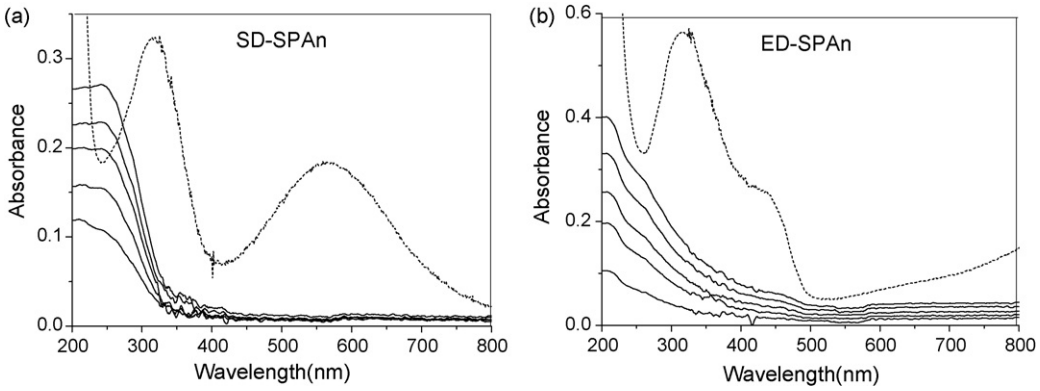

Fig. 1. UV–vis absorption spectra of LBL films fabricated on quartz plates. The number of bilayers is 2, 4, 6, 8 and 10 from the bottom to top: (a) SD-SPAn/TiO_2 LBL films and (b) ED-SPAn/TiO_2 LBL films. The spectra of aqueous solution are shown in dash line, respectively.

of polyaniline backbone, and the weak absorption at ~600 nm can be ascribed to the "exciton" transition. In ED-SPAn aqueous solution, the peaks at 320 and 436 nm are attributed to the $\pi \rightarrow \pi^*$ transition and the polaron band transition of ED-SPAn, respectively [24]. Such results suggest that SPAn changes its form from protonated emeraldine in aqueous solution to emeraldine base in the ED-SPAn/TiO_2 LBL films.

In both the SPAn/TiO_2 LBL films, the $\pi \rightarrow \pi^*$ transition of SPAn has a blue shift relative to that in SPAn solutions. Similar result was reported that the peak at 340 nm of polyaniline shifted to 318 nm of polyaniline/TiO_2 nanocomposite [18]. This is because that the extent of π-conjugation in polyaniline backbone was reduced due to the interaction between SPAn and TiO_2, resulting in the blue shifts of the absorption bands. The formation of chelate bonding between sulfonate groups and titanium atoms will also result in the destruction of polarons in two kinds of SPAn, which is responsible of the disappearance of the polaron band transitions in both the LBL films. Although both the LBL films were fabricated finally in acidic media, SPAn is in its emeraldine base form. This phenomenon is quite different with the polyaniline/TiO_2 films prepared chemically or electrochemically, in which polyaniline is conducting [31].

In Fig. 2, the absorbance at 215, 245, 207 and 260 nm increases uniformly with the bilayer number, which indicates that a progressive assembly runs regularly with almost equal amount of deposition in each cycle. Thus, the linear fabrication process is successful and consistent for both SPAn and TiO_2 in two cases.

3.3. AFM images

Fig. 3 shows AFM images of five-bilayer nanocomposite LBL films deposited on silicon wafers. Both the TiO_2 layers exhibit a microscopic structure formed from nanometer-scale grains with uniformity in both the films. However, the morphology of ED-SPAn/TiO_2 LBL films is evener than that of SD-SPAn/TiO_2 LBL films, and the size of TiO_2 nanoparticles in ED-SPAn/TiO_2 LBL films is finer than that in SD-SPAn/TiO_2 LBL films. This result is consistent with UV–vis absorption spectroscopic measurements. According to the AFM images, the particles in SPAn/TiO_2 films prepared using self-assembly technique is more uniform than PANI–TiO_2 nanocomposite particles fabricated with other methods [15,18].

3.4. Cyclic voltammetric measurements

Fig. 4 shows cyclic voltammograms (CVs) of two kinds of SPAn/TiO_2 LBL films in 0.1 M KCl solution (pH 7) at scan rate of 100 mV s^{-1}. Although SPAn is in its emeraldine base form in both the SPAn/TiO_2 LBL films, its electrochemical behaviours are quite distinct in both the cases, which should be ascribed to the difference in the fabrication materials and methods.

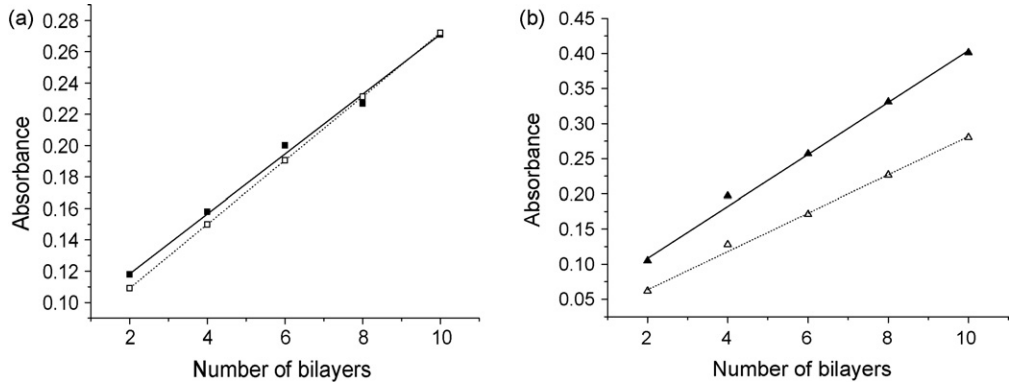

Fig. 2. The relationship between absorption and the number of bilayers: (a) SD-SPAn/TiO_2 LBL films and (b) ED-SPAn/TiO_2 LBL films. (■) At 215 nm; (□) at 245 nm; (▲) at 207 nm; (△) at 260 nm.

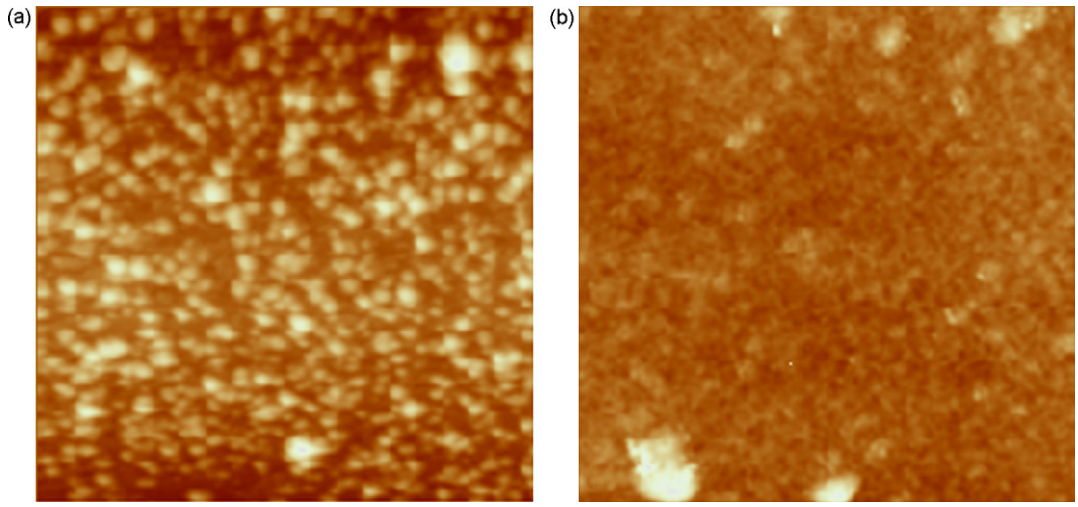

Fig. 3. AFM images of five-bilayer SPAn/TiO_2 films (TiO_2 on the outermost layer): (a) SD-SPAn/TiO_2 LBL films and (b) ED-SPAn/TiO_2 LBL films. The dimension of both the images is 3 μm × 3 μm.

Cyclic voltammogram of SD-SPAn films in 1 M HCl consists of two redox peaks: the first peak has an $E_{1/2} = 0.28$ V and the second has an $E_{1/2} = 0.77$ V versus saturated Ag/AgCl [23]. When pH value increases, the peaks shift to low potential values. When pH reaches 7, the first redox peak disappears, and the second peak has an $E_{1/2}$ value of 0.15 V [23]. In Fig. 4a, the CV of SD-SPAn/TiO_2 LBL films consists of an anodic peak at −0.02 V and two cathodic peaks at −0.3 and ∼0 V versus Ag/AgCl. This characteristic is in contrast to that of SPAn films measured in 0.3 M Na_2SO_4 solution (pH 7) at the scan rate of 60 mV s^{-1} [26]. In the latter case, there is an anodic peak at 0.25 V and two cathodic peaks at −0.1 and 0.34 V versus SCE. The peak-potentials of SPAn/TiO_2 LBL films are lower than those of SPAn films at pH 7, which can be ascribed to the interaction between SD-SPAn and TiO_2 nanoparticles. The anodic peak decreases in the second and third scan time, which indicates that the SD-SPAn/TiO_2 LBL films are not steady in KCl solution.

It was reported that when pH value was larger than 5, where the quinoid units in ED-SPAn began to appear, the anodic peak-potential (E_{ap}) values were constant at 0.44 V versus Ag/AgCl, and the cathodic peak was not observed [25]. In the ED-SPAn/TiO_2 LBL films, the CV only has an anodic peak shifting to −0.32 V at pH 7 (Fig. 4b), which shifts to low potential as compared with that of ED-SPAn. This shift should be relative to the chelate bonding between ED-SPAn and titanium atom.

In both the nanocomposite films, the redox process of SPAn follows an electron–proton transfer mechanism and show similar electrochemical behaviours to their parent sulfonated polyanilines [23,33], indicating that the electrochemical characteristics of SPAn were not significantly changed by the presence of TiO_2 in both the cases. Owing to the interaction between sulfonate groups and TiO_2 nanoparticles, less energy is needed to remove the electrons from SPAn chain during the redox processes and consequently peak-potentials decrease in both the LBL films [34].

3.5. Photocurrent responses

The photocurrent responses of ITO electrodes covered with five-bilayer SPAn/TiO_2 LBL films were shown in Fig. 5. The photoresponses of two kinds of LBL films are quite different.

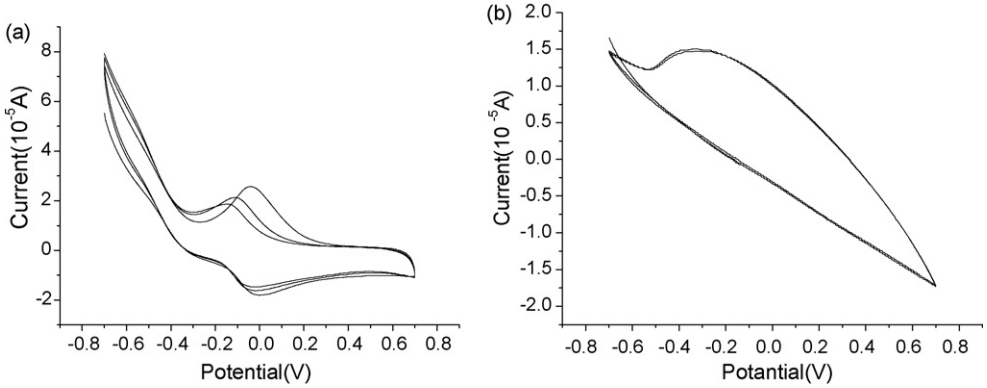

Fig. 4. Cyclic voltammograms of five-bilayer SPAn/TiO_2 LBL films on ITO glass plates at 100 mV/s: (a) SD-SPAn/TiO_2 LBL films and (b) ED-SPAn/TiO_2 LBL films.

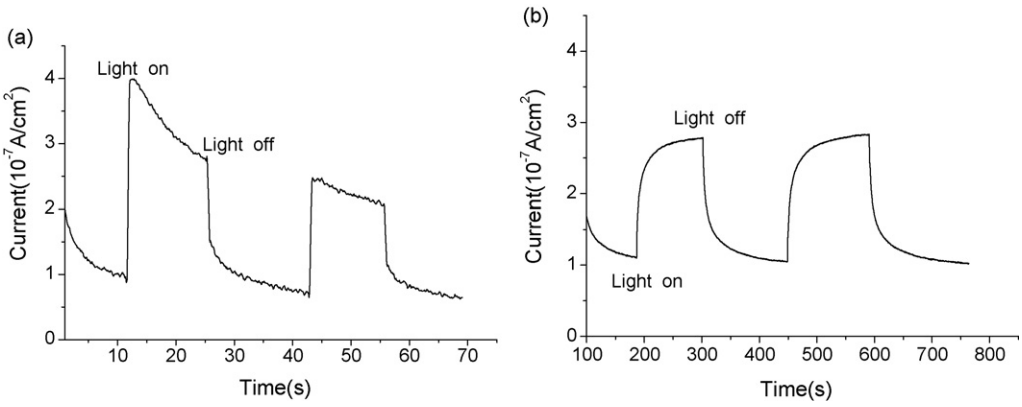

Fig. 5. Photocurrent responses of five-bilayer SPAn/TiO_2 LBL films: (a) SD-SPAn/TiO_2 LBL films and (b) ED-SPAn/TiO_2 LBL films. The potential of the working electrode was set at 0.0 V vs. the Pt counter electrode.

The SD-SPAn/TiO_2 LBL films show a fast and bigger but unstable photocurrent response, whereas the ED-SPAn/TiO_2 LBL films show a slow but stable one. The former is not stable in KCl solution due to the high ionic strength of this electrolyte [32]. The ED-SPAn/TiO_2 LBL films have slow response and recovery times. The reason is that the size of TiO_2 particles in ED-SPAn/TiO_2 film is smaller so most of electron–hole pairs are generated sufficiently close to the surface. They may quickly reach the surface, and undergo rapid surface recombination due to the lack of driving force for electron–hole pair separation [35]. The surface recombination can make the photocurrent response slower [36]. However, such films show a stable photocurrent response, which is associated with the close contact between ED-SPAn and the fine TiO_2 nanoparticles derived from $TiCl_4$.

In our case, the photocurrent is generated when protons are absorbed by SPAn at the SPAn–TiO_2 interface, and subsequently the excited SPAn molecules transfer the electrons into the conduction band of TiO_2 nanoparticles. In this way, the morphology of interface is important to the generation of photocurrent.

4. Conclusions

In conclusion, we have fabricated two kinds of SPAn/TiO_2 nanocomposite ordered ultrathin films on various substrates by the layer-by-layer self-assembly technique. The optical and electrochemical properties of two kinds of LBL films are quite different. AFM images reveal that TiO_2 is dispersed in the polymer films as very fine nanoparticles and the size of TiO_2 particles in ED-SPAn/TiO_2 LBL films is smaller than that in SD-SPAn/TiO_2 LBL films. Cyclic voltammograms show that SD-SPAn/TiO_2 LBL films have an expressed electrochemical activity in 0.1 M KCl solution than ED-SPAn/TiO_2 LBL films. The SD-SPAn/TiO_2 LBL films show a fast but unstable photocurrent response, whereas the ED-SPAn/TiO_2 LBL films show a slow but stable one. This work is well conduced to comprehend the differences between SD-SPAn and ED-SPAn. By optimizing the preparation conditions and film parameters, the two kinds of nanocomposites could be used in photoelectrochemical applications.

Acknowledgments

The authors thank the financial supports from Shanghai Rising-Star Program (03QB14015) and the Excellent Young Teachers Program of MOE, PR China.

References

[1] Y. Lu, R. Ganguli, C.A. Drewien, M.T. Anderson, C.J. Brinker, W. Gong, Y. Guo, H. Soyez, B. Dunn, M.H. Huang, J.I. Zink, Nature 389 (1997) 364.
[2] H.M. Ding, M.K. Ram, C. Nicolini, J. Mater. Chem. 12 (2002) 1.
[3] W. Feng, T. Umeda, A. Fujii, X. Wang, K. Yoshino, Jpn. J. Appl. Phys. 43 (6A) (2004) 3473.
[4] D. Chowdhury, A. Paul, A. Chattopadhyay, Langmuir 21 (2005) 4123.
[5] S.J. Su, N. Kuramoto, Synth. Met. 114 (2000) 147.
[6] S. Maeda, S.P. Armes, Chem. Mater. 7 (1995) 171.
[7] S.H. Jang, M.G. Han, S.S. Im, Synth. Met. 110 (2000) 17.
[8] Y.J. Wang, X.H. Wang, J. Li, Z.S. Mo, X.J. Zhao, X.B. Jing, F.S. Wang, Adv. Mater. 13 (2001) 1582.
[9] F. Huguenin, M. Ferreira, V. Zucolotto, F.C. Nart, R.M. Torresi, O.N. Oliveira Jr., Chem. Mater. 16 (2004) 2293.
[10] M.X. Wan, W.X. Zhou, J.C. Li, Synth. Met. 78 (1996) 27.
[11] D.C. Schnitzler, A.J.G. Zarbin, J. Braz. Chem. Soc. 15 (2004) 378.
[12] N.I. Kovtyukhova, T.E. Mallouk, Adv. Mater. 17 (2) (2005) 187.
[13] N.I. Kovtyukhova, B.R. Martin, J.K.N. Mbindyo, T.E. Mallouk, M. Cabassi, T.S. Mayer, Mater. Sci. Eng. C C19 (1–2) (2002) 255.
[14] M.K. Ram, O. Yavuz, V. Lahsangah, M. Aldissi, Sens. Actuators B: Chem. B 106 (2) (2005) 750.
[15] P.R. Somani, R. Marimuthu, U.P. Mulik, S.R. Sainkar, D.P. Amalnerkar, Synth. Met. 106 (1999) 45.
[16] I.S. Lee, J.Y. Lee, J.H. Sung, H.J. Choi, Synth. Met. 152 (1–3) (2005) 173.
[17] K. Gurunathan, D.P. Amalnerkar, D.C. Trivedi, Mater. Lett. 57 (9–10) (2003) 1642.
[18] W. Feng, E. Sun, A. Fujii, H. Wu, K. Niihara, K. Yoshino, Bull. Chem. Soc. Jpn. 73 (11) (2000) 2627.
[19] L. Zhang, M. Wan, Y. Wei, Synth. Met. 151 (1) (2005) 1.
[20] X. Sui, Y. Chu, S. Xing, M. Yu, C. Liu, Colloid Surf. A 251 (1–3) (2004) 103.
[21] L. Zhang, M. Wan, J. Phys. Chem. B 107 (28) (2003) 6748.
[22] J. Yue, A.J. Epstein, J. Am. Chem. Soc. 112 (1990) 2800.
[23] J. Yue, Z.H. Wang, K.R. Cromack, A.J. Epstein, A.G. MacDiarmid, J. Am. Chem. Soc. 113 (1991) 2665.
[24] S. Ito, K. Murata, S. Teshima, S. Teshima, R. Aizawa, Y. Asako, K. Takahashi, B.M. Hoffman, Synth. Met. 96 (1998) 161.
[25] K. Takahashi, K. Nakamura, T. Yamaguchi, T. Komura, S. Ito, R. Aizawa, K. Murata, Synth. Met. 128 (2002) 27.
[26] C.M. Li, S.L. Mu, Synth. Met. 149 (2005) 143.

[27] G. Decher, J.D. Hong, Ber. Bunsenges. Phys. Chem. 95 (1991) 1430.
[28] I. Ichinose, H. Senzu, T. Kunitake, Chem. Mater. 9 (1997) 1296.
[29] J.M. Yeh, S.J. Liou, C.Y. Lai, P.C. Wu, Chem. Mater. 13 (2001) 1131.
[30] L.E. Brus, J. Chem. Phys. 79 (1983) 5566.
[31] A. Dey, S. De, A. De, S.K. De, Nanotechnology 15 (2004) 1277.
[32] T.B. Cao, L.H. Wei, S.M. Yang, M.F. Zhang, C.H. Huang, W.X. Cao, Langmuir 18 (2002) 750.
[33] J. Yue, A.J. Epstein, J. Chem. Soc., Chem. Commun. 21 (1992) 1540.
[34] X.L. Wei, Y.Z. Wang, S.M. Long, C. Bobeczko, A.J. Epstein, J. Am. Chem. Soc. 118 (1996) 2545.
[35] Z.B. Zhang, C.C. Wang, R. Zakaria, J.Y. Ying, J. Phys. Chem. B 102 (1998) 10871.
[36] L.M. Peter, J. Li, R. Peat, J. Electroanal. Chem. 165 (1984) 29.